



## SO<sub>2</sub>-induced stability of Ag-alumina catalysts in the SCR of NO with methane

X. She <sup>a,b</sup>, M. Flytzani-Stephanopoulos <sup>a,\*</sup>, C. Wang <sup>b</sup>, Y. Wang <sup>b</sup>, C.H.F. Peden <sup>b</sup>

<sup>a</sup> Department of Chemical and Biological Engineering, Tufts University, Medford, MA, USA

<sup>b</sup> Institute for Interfacial Catalysis, Pacific Northwest National Laboratory, Richland, WA, USA

### ARTICLE INFO

#### Article history:

Received 13 June 2008

Received in revised form 14 September 2008

Accepted 19 September 2008

Available online 27 September 2008

#### Keywords:

Silver catalyst

Alumina

Sintering

Dispersion

SO<sub>2</sub>

SCR of NO

CH<sub>4</sub>

NO<sub>x</sub> reduction

### ABSTRACT

We report on a stabilization effect on the structure and activity of Ag/Al<sub>2</sub>O<sub>3</sub> for the selective catalytic reduction (SCR) of NO<sub>x</sub> with CH<sub>4</sub> imparted by the presence of SO<sub>2</sub> in the exhaust gas mixture. The reaction is carried out at temperature above 600 °C to keep the surface partially free of sulfates. In SO<sub>2</sub>-free gases, catalyst deactivation is fast and measurable at these temperatures. Time-resolved TEM analyses of used samples have determined that deactivation is due to sintering of silver from well-dispersed clusters to nanoparticles to micrometer-size particles with time-on-stream at 625 °C. However, sintering of silver was dramatically suppressed by the presence of SO<sub>2</sub> in the reaction gas mixture. The structural stabilization by SO<sub>2</sub> was accompanied by stable catalyst activity for the NO reduction to N<sub>2</sub>. The direct oxidation of methane was suppressed, thus the methane selectivity was improved in SO<sub>2</sub>-laden gas mixtures. In tests with high-content silver alumina with some of the silver present in metallic form, an increase in the SCR activity was found in SO<sub>2</sub>-containing gas mixtures. This is attributed to redispersion of the silver particles by SO<sub>2</sub>, an unexpected finding. The catalyst performance was reversible over many cycles of operation at 625 °C with the SO<sub>2</sub> switched on and off in the gas mixture.

© 2008 Elsevier B.V. All rights reserved.

## 1. Introduction

Silver catalysts have found unique application to ethylene epoxidation [1,2] and hold great promise for the SCR of NO<sub>x</sub> with hydrocarbons [3,4]. However, sintering is a serious issue for silver catalysts [5–10], and a complex array of factors have been linked to sintering, including the reaction gas environment [7,8], support effects [11], and surface binding and mobility [12]. Insights into silver growth and agglomeration mechanisms have been gained primarily from investigations of model silver catalyst systems, such as Ag films [5,6] and model Ag-alumina systems [7,11,13]. Presland et al. [5,6] have observed agglomeration of silver on annealing a silver film in oxygen, which was accompanied with the formation of hillocks and pits. It was proposed that silver migrates via surface diffusion which is enhanced by the presence of oxygen [14–17]. The appearance of big Ag clusters was found at much lower loadings than Mn on Al<sub>2</sub>O<sub>3</sub>/Ni<sub>3</sub>Al(1 1 1) surface by STM [13]. Bird et al. [11] investigated the growth of silver on model Ag-alumina catalysts by AFM (atomic force microscopy), and found that the structure and stability of silver deposits have a strong dependence on the crystalline structure of alumina. Ruckenstein

and Lee [7] performed an extensive microscopy study of the sintering behavior of model Ag/Al<sub>2</sub>O<sub>3</sub> catalysts in O<sub>2</sub>, C<sub>2</sub>H<sub>4</sub> or C<sub>2</sub>H<sub>4</sub>/O<sub>2</sub>, and found that the stability of silver depends strongly on the reaction gas environment.

Using DFT, Meyer et al. [12] examined silver bonding to various Al<sub>2</sub>O<sub>3</sub> surfaces, and found that stronger bonding exists with the O-terminated than with the Al-terminated surfaces. As a consequence, the diffusion barrier for silver is higher on the former surface than on the latter. The strength of Ag bonding to hydroxylated alumina surfaces was calculated to be intermediate between O-terminated and Al-terminated surfaces. Similar to the above model catalysts, Seyedmonir et al. [8] found that for supported silver catalysts, silver sintering also depends on the support material and the gaseous environment. The dispersion of silver was measured with a number of complementary characterization methods, including H<sub>2</sub>-titration, O<sub>2</sub>-chemisorption, XRD and TEM. Oxygen causes significant silver sintering on Ag/SiO<sub>2</sub>, while the effect is much milder for Ag/γ-Al<sub>2</sub>O<sub>3</sub> and nearly no effect was measured on Ag/TiO<sub>2</sub>. Pretreatment in H<sub>2</sub> or He does not affect the silver dispersion on these catalysts. It was also pointed out that once sintered, silver cannot be redispersed by oxygen or chlorine, unlike metals like Pt [18].

Recently, silver catalysts have attracted a lot of attention for potential application in the selective catalytic reduction (SCR) of NO<sub>x</sub> by hydrocarbons or oxygenates to remove nitrogen oxides from various exhaust gas effluents [3,4,19–21]. Their promise lies

\* Corresponding author.

E-mail address: [maria.flytzani-stephanopoulos@tufts.edu](mailto:maria.flytzani-stephanopoulos@tufts.edu)  
(M. Flytzani-Stephanopoulos).

in their high activity, high selectivity to dinitrogen, and moderate resistance to  $\text{H}_2\text{O}$  and  $\text{SO}_2$ . In previous work with Ag-alumina catalysts prepared by the coprecipitation-gelation [19,20], rather unexpectedly, we found that the presence of high concentrations of  $\text{SO}_2$  ( $\sim 1000$  ppm) stabilized the catalyst activity for  $\text{CH}_4$ -SCR of NO at  $625^\circ\text{C}$  and suppressed the catalyst deactivation observed in the absence of  $\text{SO}_2$  [21]. In this paper, we further probe the reasons for the observed stability by detailed characterization of Ag-alumina catalysts aged in the absence or presence of  $\text{SO}_2$ . We also followed the effect of  $\text{SO}_2$  on the activity and stability of high-content Ag/ $\text{Al}_2\text{O}_3$  materials in which part of the silver is present as metallic nanoparticles.

## 2. Experimental

A coprecipitation-gelation (co-gel) method was used to prepare Ag-alumina catalysts in this work as described in [19]. Low-silver content Ag-alumina catalysts were prepared by leaching out the weakly bound silver on the parent catalysts with a dilute (10%) nitric acid solution [20]. These two types of catalysts are denoted as  $\text{AlAg}(x,\text{CG})$  and  $\text{AlAg}(x,\text{L})$ , respectively, where  $x$  is the wt% of silver, CG stands for coprecipitation-gelation preparation and L for leaching.

Catalytic activity measurements were carried out in a fixed-bed quartz (1 cm I.D.) flow reactor equipped with a K-type thermocouple and a temperature controller, as described elsewhere [19,20]. Specifically,  $\sim 0.15$  g powder samples were loaded into the reactor, and a feed gas stream containing (mol%)  $0.25\text{NO-2CH}_4-5\text{O}_2-0$  or  $0.1\text{SO}_2\text{-balHe}$  at  $200\text{ ml/min}$  ( $\text{GHSV} = 50,000\text{ h}^{-1}$ ) was introduced. Typically, the reaction took place at  $625^\circ\text{C}$  at atmospheric pressure. At this (or higher) temperature, the catalyst surface is only partially sulfated and active for  $\text{CH}_4$ -SCR of NO even in the presence of  $\text{SO}_2$  in the gas [21]. The reactor effluent was analyzed by a gas chromatograph (HP 5890), which was equipped with a thermal conductivity detector (TCD) and a  $10\text{ ft long} \times 1/8\text{ in. diameter}$  5A molecular sieve column capable of separating  $\text{NO}$ ,  $\text{CH}_4$ ,  $\text{O}_2$ ,  $\text{N}_2$  and  $\text{CO}$  species. An FTIR (Mattson, Research Series 1), equipped with a  $0.75\text{ l}/5.6\text{ m}$  gas cell operating at  $150^\circ\text{C}$ , was used to monitor the  $\text{SO}_2$  concentration online.

Ag-alumina samples, both fresh and reaction-aged, were examined by HRTEM/EDS on a JEOL 2010 instrument equipped with a  $\text{LaB}_6$  electron gun source with a resolution of  $0.19\text{ nm}$ . The microscope was operated at  $200\text{ kV}$ , and its attached energy dispersive X-ray spectroscopy (EDS) was also used for elemental analysis of selected areas. The sample preparation consisted of suspending the catalyst powders in isopropyl alcohol using an ultrasonic bath and then depositing them onto a carbon-coated 200 mesh Cu grid. Typically, for each sample, the particle size distribution was investigated over many areas of the samples, and representative pictures are shown here.

To identify the crystalline phases, X-ray powder diffraction (XRD) analysis was performed on a Rigaku 300 X-ray diffractometer. Copper  $\text{K}\alpha$  radiation was used. The tube voltage was  $60\text{ kV}$ , and the current was  $300\text{ mA}$ .

TPO (temperature-programmed oxidation) was performed to check for carbon deposition on the Ag-alumina catalysts aged in either of the following two conditions: (1) sulfur-free:  $625^\circ\text{C}$ ,  $0.25\text{NO-2CH}_4-5\text{O}_2\text{-He}$ , 24 h; and (2) with sulfur:  $625^\circ\text{C}$ ,  $0.25\text{NO-2CH}_4-5\text{O}_2-0.1\text{SO}_2\text{-He}$ , 24 h. Three catalysts,  $\text{AlAg}(6,\text{L})$ ,  $\text{AlAg}(10.1,\text{CG})$  and alumina, were examined. TPO was performed on a Micromeritics Pulse Chemisorb 2705 instrument. Typically,  $\sim 0.1$  g of aged catalyst was charged into the U-shape sample holder, and  $20\text{O}_2/\text{He}$  at  $40\text{ ml/min}$  was introduced at RT. Then the sample was heated in this flowing gas mixture to  $800^\circ\text{C}$  at  $10^\circ\text{C}/\text{min}$ . Signals of  $\text{O}_2(32,16)$ ,  $\text{CO}(28)$ ,  $\text{CO}_2(44,28)$  and  $\text{H}_2\text{O}(18)$  were monitored by mass

spectrometry, as well as some S- or N-containing species:  $\text{NO}(30)$ ,  $\text{NO}_2(46)$ ,  $\text{N}_2\text{O}(44)$ ,  $\text{SO}_2(64,48)$ ,  $\text{SO}_3(80)$ ,  $\text{H}_2\text{S}(34)$ ,  $\text{COS}(60)$ ,  $\text{CS}_2(76)$  and  $\text{CH}_2\text{S}(45)$ . For the MS signal of  $\text{CO}$  ( $m/e = 28$ ),  $0.12$  of the  $\text{CO}_2(44)$  signal was subtracted to account for  $\text{CO}$  produced by  $\text{CO}_2$  cracking in the mass spectrometer ionizer. Similarly, for the  $m/e$  signal of  $\text{NO}$  (30),  $2.7$  times the signal of  $\text{NO}_2$  (46) was subtracted to account for the  $\text{NO}$  produced from  $\text{NO}_2$  whenever these two components showed up simultaneously.

$\text{SO}_2$  treatment of a pre-sintered Ag-alumina catalyst was conducted to examine whether  $\text{SO}_2$  can redisperse silver particles. The sample,  $\text{AlAg}(10.1,\text{CG})$ , was first aged in sulfur-free  $\text{CH}_4$ -SCR reaction (standard condition:  $0.25\text{NO-2CH}_4-5\text{O}_2$ ) at  $625^\circ\text{C}$  for 24 h. This aged catalyst is denoted as  $\text{AlAg}(10.1,\text{CG})(625\text{C-SCR-24 h})$ . Sulfation of this  $\text{CH}_4$ -SCR-aged catalyst was performed in a fixed bed quartz flow reactor. Firstly, the sample was heated from RT to  $625^\circ\text{C}$  in He. Then, sulfation was performed in a flow of  $516\text{ ppm SO}_2/\text{He}$  at  $625^\circ\text{C}$  for specific lengths of time. Finally, the catalyst was cooled down to RT in the same  $\text{SO}_2$  gas stream. The gas effluent from the reactor was monitored with a mass spectrometer (Mini-Lab). The sulfated catalyst was examined by TEM (JEOL 2010) and XRD (Philips, X'pert) to determine the dispersion and crystalline phases of silver.

## 3. Results and discussion

### 3.1. $\text{SO}_2$ -stabilized $\text{CH}_4$ -SCR activity of Ag-alumina

A most interesting property of the catalyst in the presence of  $\text{SO}_2$  is the stabilization of its activity as we recently reported [21]. Fig. 1 shows this in a cyclic addition/removal of  $\text{SO}_2$  over the  $\text{AlAg}(6,\text{L})$  catalyst. Clearly, addition of  $\text{SO}_2$  causes a fast drop in the conversions of  $\text{NO}$  and  $\text{CH}_4$ , which are subsequently recovered after removal of  $\text{SO}_2$ . We have attributed this to reversible adsorption of  $\text{SO}_2$  onto the surface sites of Ag-alumina at  $625^\circ\text{C}$  [21]. What is remarkable is the stabilizing effect of  $\text{SO}_2$  on the SCR activity of  $\text{AlAg}(6,\text{L})$ , as can be seen in Fig. 1. Under  $\text{SO}_2$ , both the  $\text{NO}$  conversion to  $\text{N}_2$  and  $\text{CH}_4$  conversion to  $\text{CO}_x$  were stable with time (up to  $18\text{ h}$  of time-on-stream). On the contrary, in the absence of  $\text{SO}_2$  from the reaction gas mixture, a continuous drop in  $\text{NO}$  conversion was found. For example, after the last cycle in Fig. 1, when  $\text{SO}_2$  was switched off the conversion of  $\text{NO}$  to  $\text{N}_2$  decreased from  $82$  to  $32\%$  in  $18\text{ h}$ , while the conversion of  $\text{CH}_4$  to  $\text{CO}_x$  was maintained with time.

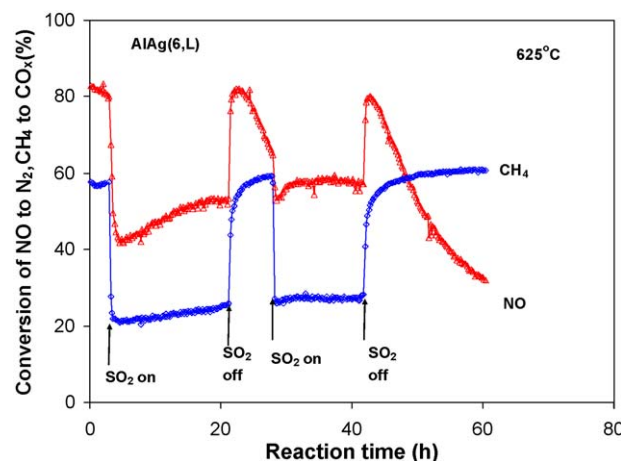


Fig. 1. Effect of  $\text{SO}_2$  on the SCR of NO with  $\text{CH}_4$  over  $\text{AlAg}(6,\text{L})$ . Catalyst load:  $0.15\text{ g}$ . Feed gas:  $0.25\text{NO-2CH}_4-5\text{O}_2-0/1000\text{ ppm SO}_2\text{-He}$ ,  $200\text{ ml/min}$ .  $T = 625^\circ\text{C}$ .  $\text{SV} = 50,000\text{ h}^{-1}$ .

As a result, the aim of this work was to investigate the role played by potential structural changes of silver on (1) the deactivation of Ag-alumina catalysts in the absence of  $\text{SO}_2$ ; and (2) the enhanced stability of Ag-alumina in the presence of  $\text{SO}_2$ .

### 3.2. Deactivation in $\text{SO}_2$ -free gas streams

As shown in Fig. 1, the NO conversion to  $\text{N}_2$  decreases continuously with time-on-stream in the absence of  $\text{SO}_2$ . Sintering phenomena (e.g. silver particle growth) or fouling due to carbon deposition are the typical causes of deactivation. We first examined the catalysts for carbon deposition by subjecting them to TPO after they were aged in the absence of  $\text{SO}_2$ , no carbon deposition was evidenced from the TPO results (not shown) and this deactivation route was ruled out. For comparison, TPO was also performed for

a sample aged in the presence of  $\text{SO}_2$ , and again no evidence for carbon deposition was found.

Catalyst sintering, another common cause of catalyst deactivation, was investigated next. Silver particle sintering is known to occur readily on various supports [5–10]. To examine this, TEM was performed for the Ag-alumina catalysts aged in the absence of  $\text{SO}_2$  for various lengths of time, as shown in Fig. 2. Fig. 2(a)–(c) show the TEM of AlAg(7.1,L) aged in  $\text{CH}_4\text{-NO-O}_2$  at 625 °C for 5, 48 and 60 h, respectively. After reaction for 5 h, small silver nanoparticles of 10–20 nm average size were clear (Fig. 2(a)), indicating destabilization of silver compared to the highly dispersed [Ag-O-Al] species in the fresh sample [20]. With further reaction in the above gas mixture, growth of silver particles became more pronounced, as can be seen in Fig. 2(b) and (c). After 48 h on-stream (Fig. 2(b)), big silver agglomerates reaching

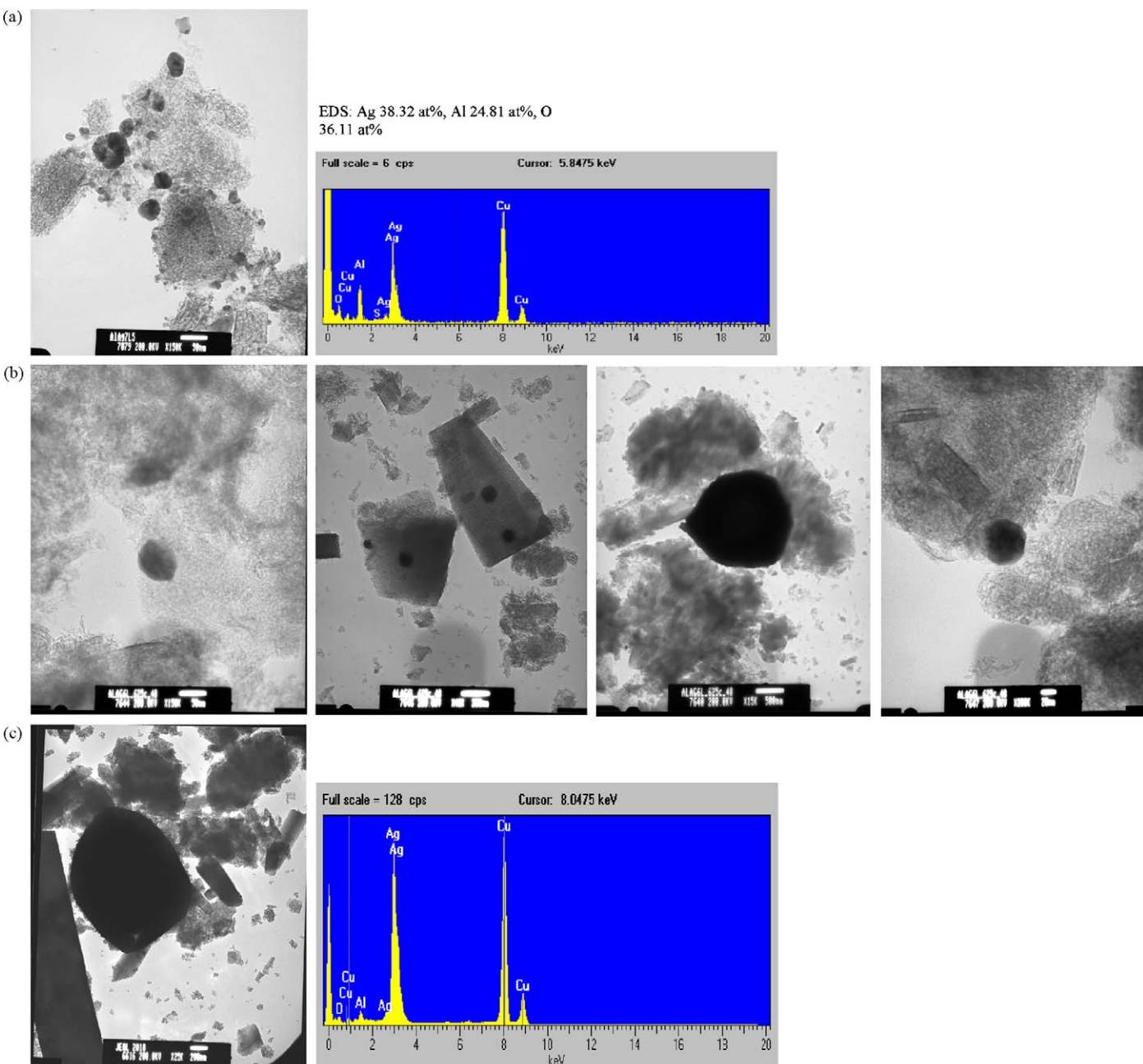


Fig. 2. HRTEM of AlAg(7.1,L) aged in the absence of  $\text{SO}_2$ . Aging condition: 0.25%NO-2% $\text{CH}_4$ -5% $\text{O}_2$ -He, 625 °C. Aging time: (a) 5 h; (b) 48 h; (c) 60 h.

micrometer size were observed, together with some smaller silver particles  $<100$  nm. A large clump of silver  $>1$   $\mu\text{m}$  was found after 60 h-on-stream (Fig. 2(c)). These results clearly show severe sintering of silver particles during the  $\text{CH}_4$ -SCR reaction at 625  $^{\circ}\text{C}$ .

Martinez-Arias et al. [22] also reported sintering of silver in Ag/alumina catalysts during  $\text{C}_3\text{H}_6$ -SCR of NO up to 550  $^{\circ}\text{C}$ .

Comparing this data to the NO conversion drop in the absence of  $\text{SO}_2$  (Fig. 1), we conclude that the observed deactivation

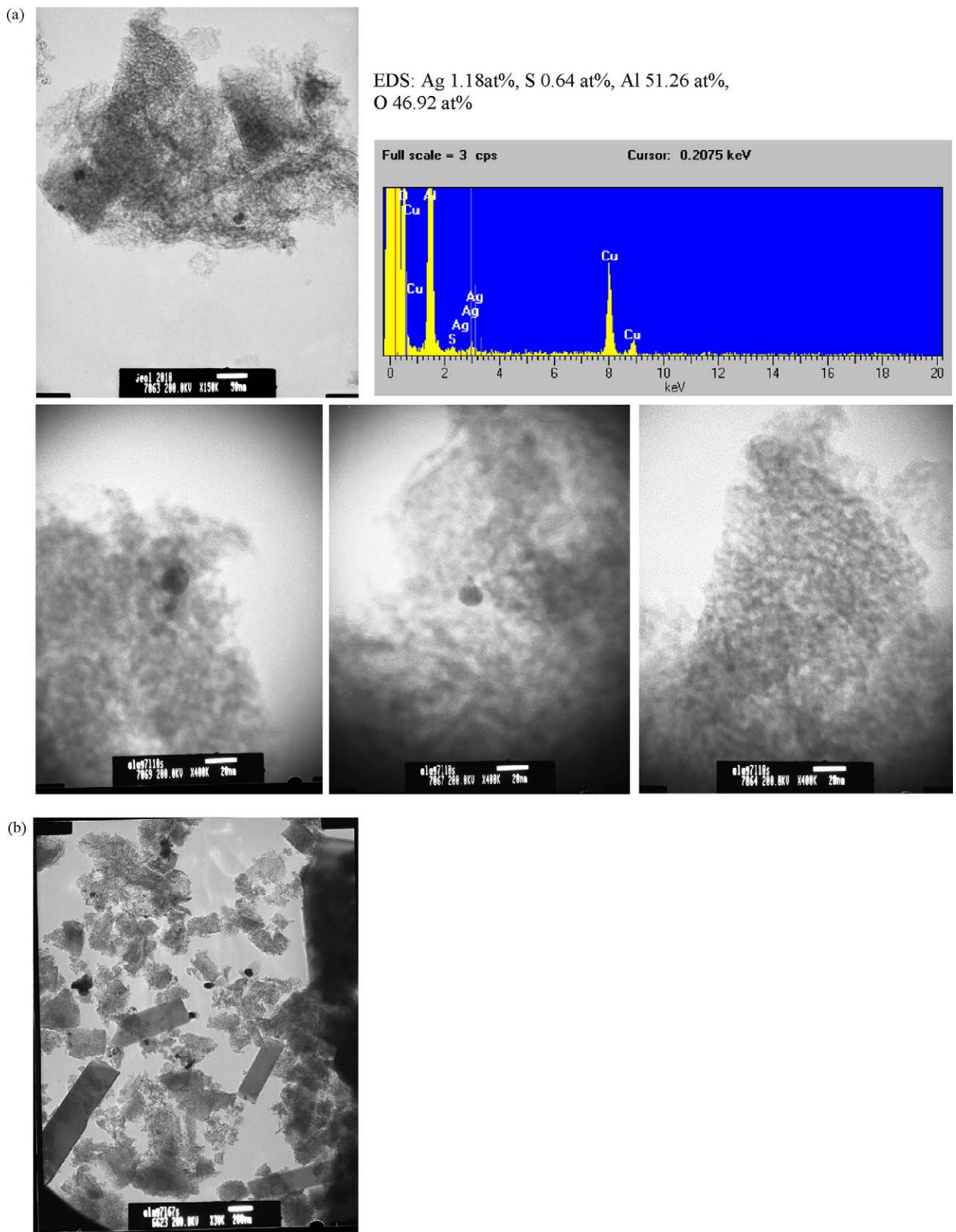


Fig. 3. HRTEM of AlAg(7.1,L) aged in the presence of  $\text{SO}_2$ . Aging condition: 0.25%NO-2% $\text{CH}_4$ -5% $\text{O}_2$ -1000 ppm  $\text{SO}_2$ -He, 625  $^{\circ}\text{C}$ . Aging time: (a) 10 h; (b) 67 h.

is due to silver sintering and hence loss of active sites for the reaction.

### 3.3. Stabilized structures and performance in the presence of $SO_2$

HRTEM was also performed with Ag-alumina samples aged in  $CH_4$ - $NO$ - $O_2$ - $SO_2$  for various times, as shown in Fig. 3. Fig. 3(a) and (b) are micrographs of AlAg(7.1,L) aged in  $CH_4$ - $NO$ - $O_2$ - $SO_2$  gas mixtures at 625 °C for 10 and 67 h, respectively. After 10 h, silver was still well dispersed and only a few particles <20 nm were observed, as can be seen in Fig. 3(a). This behavior is in sharp contrast to the case of Fig. 2(a), where the dispersion of silver was drastically lower as evidenced by the appearance of large silver particles after aging for a shorter time in the absence of  $SO_2$ . After the 67 h-test (Fig. 3(b)), a few silver particles of ~100 nm size were present, but most silver remained dispersed. This is very different from the severely sintered silver particles (>1  $\mu$ m, Fig. 2(c)) observed after aging the catalyst in the absence of  $SO_2$ . Hence, we conclude that  $SO_2$  plays an important role in suppressing the sintering of silver particles on alumina.

To examine the generality of this stabilization effect of  $SO_2$  on silver structures, we further looked at a high-silver content catalyst,

AlAg(10.1,CG), which initially contains silver nanoparticles of 10–20 nm as in Fig. 4(a). As a result of reaction at 625 °C, large silver particles reaching micrometer size were formed on this material after aging in the  $SO_2$ -free gas for 24 h (Fig. 4(b)). On the sulfated sample, however, no such severely sintered silver particles were observed, and most of the silver was well dispersed (data not shown). Therefore, the beneficial structural effect of  $SO_2$  also holds for the unleached, high-content AlAg(10.1,CG) sample.

Similar to the activity tests for the leached AlAg(6,L) in Fig. 1, the conversion of NO over AlAg(10.1,CG) decreases with time in the absence of  $SO_2$ , while it is maintained at high levels with addition of  $SO_2$ , as shown in Fig. 5. For this high-silver content catalyst, there is even an enhanced SCR activity caused by the presence of  $SO_2$ , as can be seen by the improved NO conversion to  $N_2$  in Fig. 5. Thus, we next examined the possibility that  $SO_2$  caused redispersion of the particles of silver initially present on the surface which led to this surprising enhanced activity.

### 3.4. Redispersion of silver particles by $SO_2$

XRD analyses were used to test the redispersion hypothesis. Fig. 6 shows that metallic silver were present (2 $\theta$  of 38.2° (1 1 1)

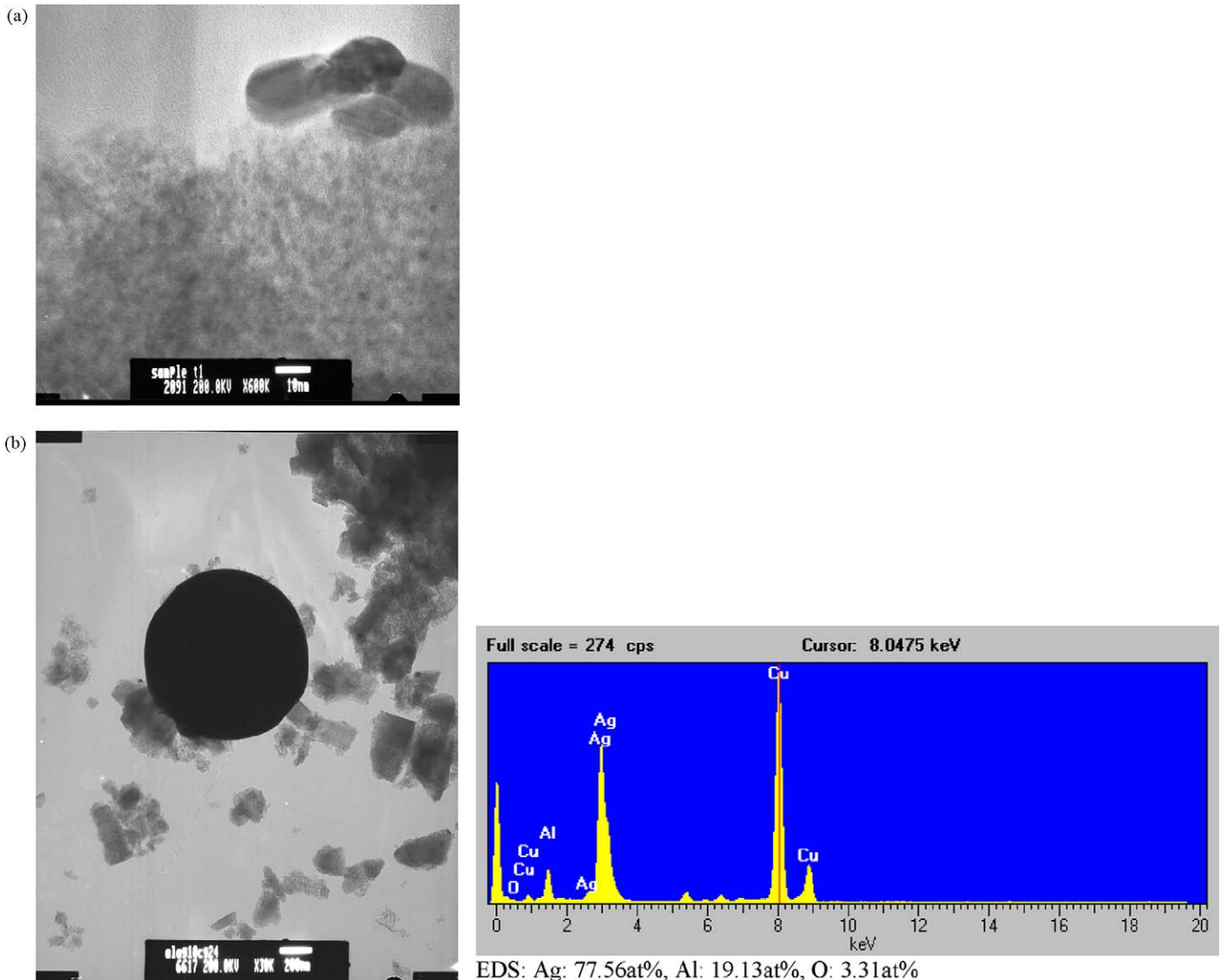
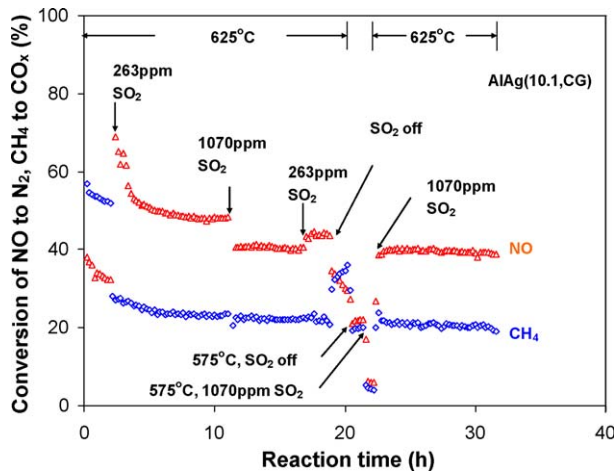
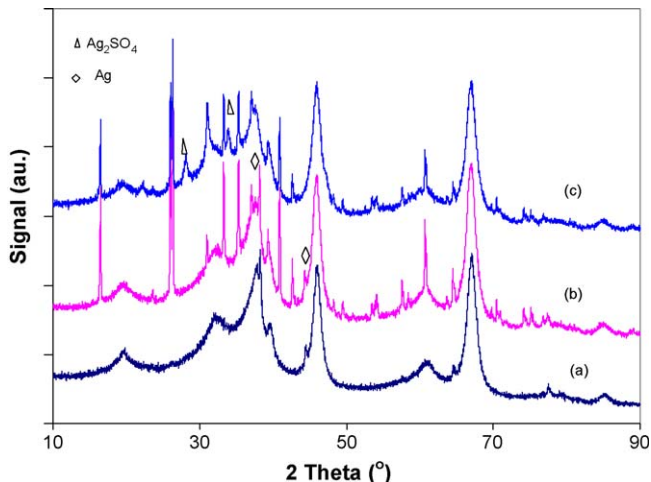


Fig. 4. HRTEM of AlAg(10.1,CG): (a) fresh; (b) aged in the absence of  $SO_2$  (625 °C, 0.25% $NO$ -2% $CH_4$ -5% $O_2$ -He, 24 h).



**Fig. 5.** Effect of  $\text{SO}_2$  on the SCR of NO with  $\text{CH}_4$  over AlAg(10.1,CG). Catalyst load: 0.15 g. Feed gas: 0.25%NO-2% $\text{CH}_4$ -5% $\text{O}_2$ -0/263/1070 ppm  $\text{SO}_2$ -He, 200 ml/min.  $T = 625$  °C.



**Fig. 6.** XRD of aged Ag-alumina catalysts. (a) AlAg(10.1,CG)(625C-SCR-24 h); (b) AlAg(7.1,L)(625C-SCR-60 h); (c) AlAg(7.1,L)(625C-SCR- $\text{SO}_2$ -67 h). Aging condition: 0.25%NO-2% $\text{CH}_4$ -5% $\text{O}_2$ -0/1000 ppm  $\text{SO}_2$ -He, 625 °C.

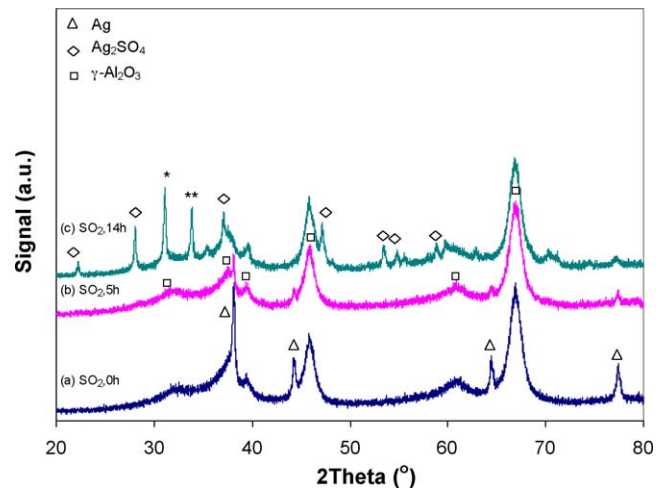


**Fig. 8.** Time-resolved XRD analysis of AlAg(10.1,CG) (625C-SCR-24 h) upon  $\text{SO}_2$  treatment (516 ppm  $\text{SO}_2$ /He at 625 °C). (a)  $\text{SO}_2$ , 0 h; (b)  $\text{SO}_2$ , 5 h (as per Fig. 7a); (c)  $\text{SO}_2$ , 14 h (as in Fig. 7b). This diffraction line cannot be unambiguously ascribed to  $\text{Ag}_2\text{SO}_4$ ,  $\text{Al}_2\text{S}_3$ , or  $\text{Al}_2\text{O}_3$ , since all three of these have diffraction line at this position.

\*Diffraction due to  $\text{Ag}_2\text{SO}_4$  or  $\text{Al}_2(\text{SO}_4)_3$ .

and 44.4° (2 0 0) for two catalysts aged in  $\text{CH}_4$ - $\text{NO}$ - $\text{O}_2$ , AlAg(7.1,L)(625C-SCR-60 h) and AlAg(10.1,CG)(625C-SCR-24 h), respectively. Based on Ag(1 1 1), the crystal size of silver on these two catalysts was calculated to be 43.6 and 38.4 nm, respectively. It should be noted that the thus obtained average crystal size by XRD was much smaller than the size of silver agglomerates identified in Fig. 2(c) and Fig. 4(b) by TEM, which could be due to the fact that XRD averages over the entire sample. When the above two catalysts were aged in  $\text{CH}_4$ - $\text{NO}$ - $\text{O}_2$ - $\text{SO}_2$  for 24 h at 625 °C, neither metallic silver nor the  $\text{Ag}_2\text{SO}_4$  phase was identified by XRD. Also shown in Fig. 6, is the XRD pattern of AlAg(7.1,L)(625C-SCR- $\text{SO}_2$ -67 h), aged in  $\text{SO}_2$  for a longer time, 67 h. No metallic silver phases exist in this sample.  $\text{Ag}_2\text{SO}_4$  was identified at  $2\theta$  of 28.2° and 34.0° and its crystal size was calculated to be 17.8 nm from the peak at 34.0°.

To further probe the hypothesis that the observed SCR activity and stability enhancement of the catalyst is due to  $\text{SO}_2$ -induced redispersion of silver, we conducted a series of experiments in which a pre-sintered Ag-alumina catalyst, AlAg(10.1,CG)(625C-

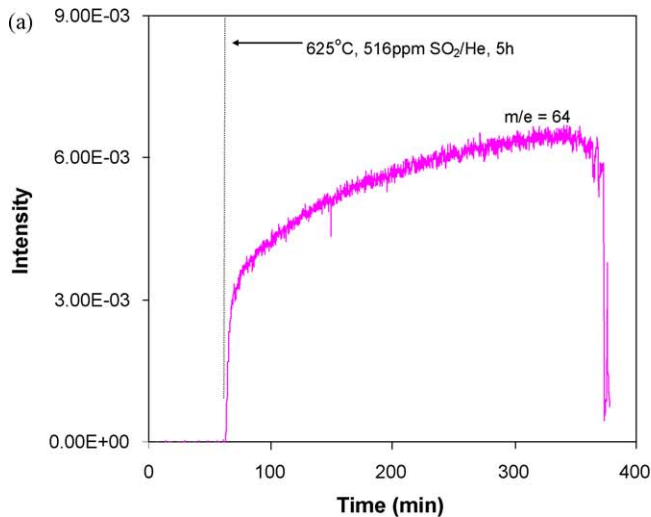


**Fig. 7.**  $\text{SO}_2$  elution monitored by mass spectrometry in two sequential  $\text{SO}_2$ -treatments (625 °C, 516 ppm  $\text{SO}_2$ /He) of AlAg(10.1,CG)(625C-SCR-24 h). (a) 5 h; (b) follows (a), 9 h.

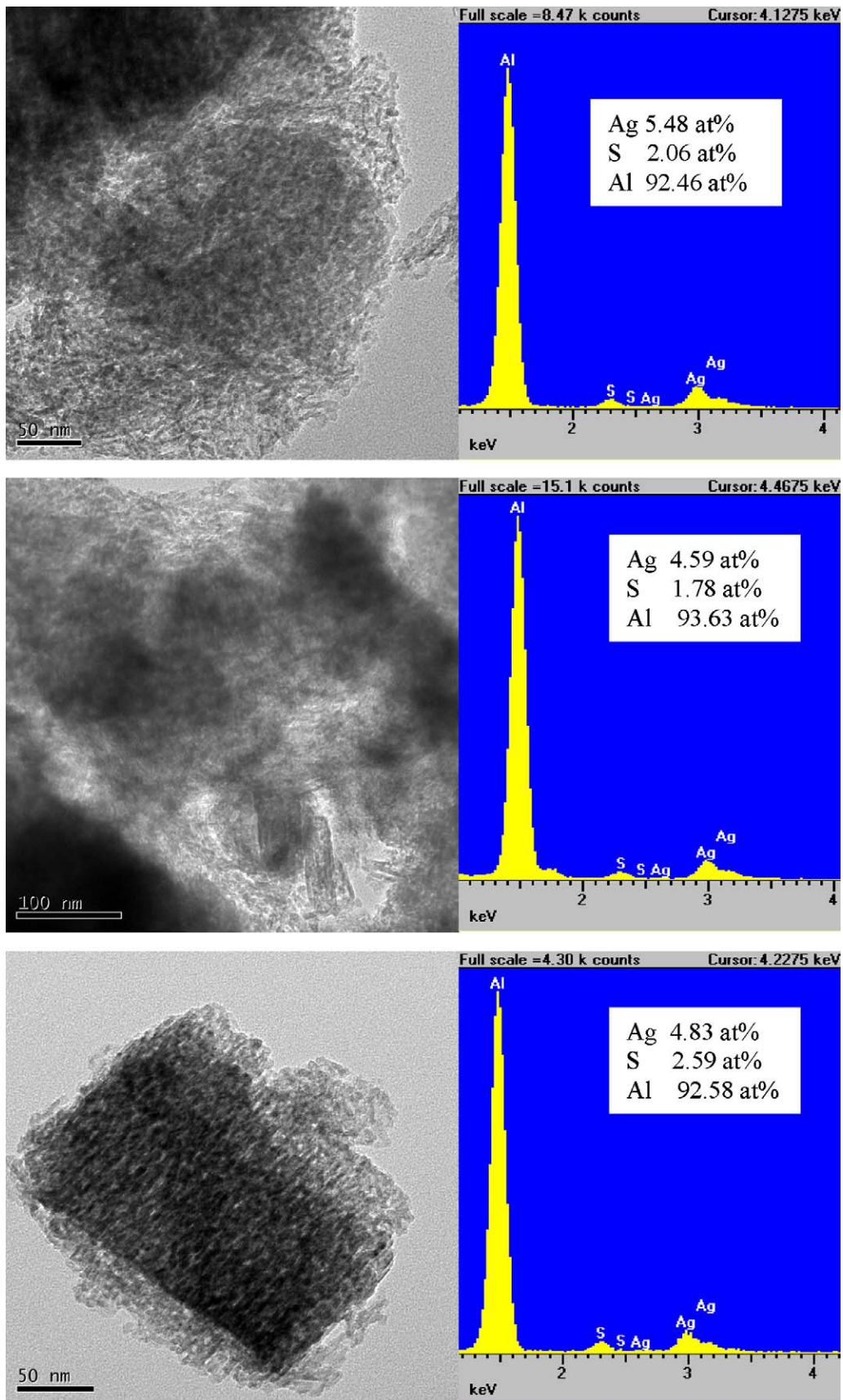


**Fig. 9.** TEM of AlAg(10.1,CG) (625C-SCR-24 h) treated in  $\text{SO}_2$  for 14 h (the sample after treatment in Fig. 7(b); 625 °C, 516 ppm  $\text{SO}_2/\text{He}$ ). EDS shows the atomic percentages of each element.

SCR-24 h) was exposed to a flow of  $\text{SO}_2$  (516 ppm  $\text{SO}_2/\text{He}$ , at 625 °C). Fig. 7 shows that the concentration of eluted  $\text{SO}_2$  gradually increases with time-on-stream, which indicates absorption of  $\text{SO}_2$  by the catalyst. The thus “sulfated” sample was characterized by XRD and TEM, as shown in Figs. 8 and 9. Fig. 8(a) shows the XRD results of the starting aged material  $\text{AlAg}(10.1,\text{CG})(625\text{C-SCR-24 h})$ , and strong diffraction lines due to metallic Ag were identified in this catalyst. After being treated in  $\text{SO}_2$  for 5 h, the intensity of those diffraction lines diminished drastically, as shown in Fig. 8(b). The metallic silver phase completely disappeared after further 9 h treatment in  $\text{SO}_2$  in Fig. 8(c), although  $\text{Ag}_2\text{SO}_4$  was identified after this extensive treatment in  $\text{SO}_2$ . Hence, the XRD results strongly support our conclusion that silver particles were redispersed by  $\text{SO}_2$ . Further, the morphology of the catalyst treated in  $\text{SO}_2$  for 14 h was examined by TEM (Fig. 9). No silver particles were identified and silver (sulfur-bounded) was well dispersed as indicated by the EDS analysis.

It is noteworthy that the saturation of the aged catalyst by  $\text{SO}_2$  takes on the order of 1–3 h as can be seen in Fig. 7. However, the redispersion of silver may have faster dynamics, when the starting sample contains smaller silver particle sizes, and when exposures occur at higher concentrations of  $\text{SO}_2$  as manifested by the relatively fast cyclic performance in Figs. 1 and 5.

To the best of our knowledge, this is the first report for a stabilization of silver on alumina surfaces by  $\text{SO}_2$  under SCR of  $\text{NO}_x$  at temperatures exceeding 600 °C.

At the present time we do not have a satisfactory model on how  $\text{SO}_2$  stabilizes and redisperses silver species on the Ag-alumina catalyst during  $\text{CH}_4$ -SCR of  $\text{NO}_x$  at temperatures above 600 °C. But our data consistently show that  $\text{SO}_2$  adsorbs reversibly on Ag-alumina under these reaction conditions [21]. Tentatively, therefore, we propose that the adsorbed  $\text{SO}_2$  can either change the bonding environment of the alumina surface and hence the bonding strength of Ag atoms [12] or form  $\text{Ag}-\text{SO}_x$  bonds that inhibit migration of silver. Along the same line, carbon deposition on silver particles by heating in  $\text{C}_2\text{H}_4$  has been reported to prevent silver from sintering [9,10]. Wang et al. [23] reported much slower nucleation of FePt particles on  $\text{FePt}/\text{ZnS}/\text{SiO}_2$  than on  $\text{FePt}/\text{SiO}_2$ , and the particle size was also much smaller in the former case. The authors explained this by the formation of Fe–S and Pt–S bonds on ZnS, which results in increased activation energies for diffusion and aggregation of FePt particles [24]. From both a mechanistic and a practical viewpoint, understanding how the stabilization of silver in dispersed state comes about by  $\text{SO}_2$  warrants further investigation. Furthermore, how  $\text{SO}_2$  can disperse already formed particles of silver on alumina at temperatures exceeding 600 °C remains an open question at the present time.

#### 4. Conclusion

The previously reported  $\text{SO}_2$ -derived stability of Ag-alumina catalysts for SCR of NO with methane at high temperatures

(>600 °C) was further investigated in this work. A beneficial structural effect of  $\text{SO}_2$  on silver is reported for the first time. In the absence of  $\text{SO}_2$ , severe sintering of silver takes place in the reaction gas at 625 °C and silver agglomerates into large clusters of  $\mu\text{m}$  size. However, the presence of  $\text{SO}_2$  keeps the silver species in a dispersed state on alumina and suppresses deactivation. Further, we found that  $\text{SO}_2$  redisperses already formed silver particles on a reaction-aged silver-alumina surface at 625 °C. As a consequence, the SCR activity of high-content  $\text{Ag}/\text{Al}_2\text{O}_3$  can be tuned to higher values by addition of  $\text{SO}_2$ , as the silver particles disappear and silver dispersion is increased. These findings are important for the treatment of engine exhaust gases containing residual sulfur.

#### Acknowledgements

This work was funded by the National Science Foundation, NIRT grant 0304515. We gratefully acknowledge the assistance of Dr. Yong Zhang of the Materials Science and Engineering Center at MIT with the TEM measurements. Part of the experiments in this work, including some of the catalyst-pretreatments, TEM and XRD measurements, were performed in the Environmental Molecular Sciences Laboratory, a national scientific user facility sponsored by the DOE Office of Biological and Environmental Research, and located at Pacific Northwest National Laboratory.

#### References

- [1] H.H. Voge, C.R. Adams, in: D.D. Eley, H. Pines, P.B. Weisz (Eds.), *Advances in Catalysis*, vol. 17, Academic Press, New York, 1967, p. 151.
- [2] D.B. Dadyburjor, S.S. Jewur, E. Ruckenstein, in: H. Heinemann, J.J. Carberry (Eds.), *Catalysis Reviews*, vol. 19, Dekker, New York, 1979, p. 293.
- [3] R. Burch, J.P. Breen, F.C. Meunier, *Appl. Catal. B* 39 (2002) 283.
- [4] K. Shimizu, *Phys. Chem. Chem. Phys.* 8 (2006) 2677.
- [5] A.E.B. Presland, G.L. Price, D.L. Trimm, *Surf. Sci.* 29 (1972) 424.
- [6] A.E.B. Presland, G.L. Price, D.L. Trimm, *Surf. Sci.* 29 (1972) 435.
- [7] E. Ruckenstein, S.H. Lee, *J. Catal.* 109 (1988) 100.
- [8] S.R. Seyedmonir, D.E. Strohmayer, G.J. Guskey, G.L. Geoffroy, M. Albert Vannice, *J. Catal.* 93 (1985) 288.
- [9] A.E.B. Presland, G.L. Price, D.L. Trimm, *J. Catal.* 26 (1972) 313.
- [10] H.K. Plummer Jr., W.L.H. Watkins, H.S. Gandhi, *Appl. Catal.* 29 (1987) 261.
- [11] D.P.C. Bird, C.M.C. de Castilho, R.M. Lambert, *Surf. Sci.* 449 (2000) L221.
- [12] R. Meyer, Q. Ge, J. Lockemeyer, R. Yeates, M. Lemanski, D. Reinalda, M. Neurock, *Surf. Sci.* 601 (2007) 134.
- [13] C. Becker, K. von Bergmann, A. Rosenhahn, J. Schneider, K. Wandelt, *Surf. Sci.* 486 (2001) L443.
- [14] M. Riassan, D.L. Trimm, P.M. Williams, *J. Chem. Soc. Faraday Trans.* 72 (1976) 925.
- [15] R.T.K. Baker, P. Skiba, *Carbon* 15 (1977) 233.
- [16] F.H. Buttner, E.R. Funk, H. Udin, *J. Phys. Chem.* 56 (1952) 657.
- [17] G.E. Rhead, *Acta Metall.* 13 (1965) 223.
- [18] S.E. Wanke, P.C. Flynn, *Catal. Rev. Sci. Eng.* 12 (1975) 93.
- [19] A. Keshavaraja, X. She, M. Flytzani-Stephanopoulos, *Appl. Catal. B* 27 (2000) L1.
- [20] X. She, M. Flytzani-Stephanopoulos, *J. Catal.* 237 (2006) 79.
- [21] X. She, M. Flytzani-Stephanopoulos, *Catal. Today* 127 (2007) 207.
- [22] A. Martínez-Arias, M. Fernández-García, A. Iglesias-Juez, J.A. Anderson, J.C. Conesa, J. Soria, *Appl. Catal. B* 28 (2000) 29.
- [23] J. Wang, K.P. Loh, Y.L. Zhong, M. Lin, J. Ding, Y.L. Foo, *Chem. Mater.* 19 (2007) 2566.
- [24] A.C.C. Yu, M. Mizuno, Y. Sasaki, M. Inoue, H. Kondo, I. Ohta, D. Djayaprawira, M. Takahashi, *Appl. Phys. Lett.* 82 (2003) 4352.